Dynamics of Polystyrene Subchains of a Styrene–Methyl Methacrylate Diblock Copolymer in Solution Measured by Dynamic Light Scattering with an Isorefractive Index Solvent. 1. Dilute Solution Region

Yoshisuke Tsunashima* and Yukinao Kawamata

Institute for Chemical Research, Kyoto University, Uji, Kyoto 611, Japan

Received February 16, 1993; Revised Manuscript Received June 5, 1993

ABSTRACT: Dynamical properties of the subchains in diblock copolymers in dilute solution were investigated by dynamic light scattering measurements on a diblock chain swollen well in a solvent isorefractive to one part of the subchains, i.e., polystyrene (PS)–poly(methyl methacrylate) (PMMA) diblock copolymer (M_w = 1.53 × 10^6, M_w/M_n = 1.01, 38.5 wt % PS) in benzene at 30 °C. Since benzene is a good solvent to both PS and PMMA and is isorefractive to PMMA, the dynamical motions of the PS subchain under the influence of the connecting PMMA part were extracted unambiguously. The dynamic structure factor observed for the visible PS subchain, $S(q,t)$, was found to be represented well by the sum of two exponentials; $S(q,t) = a_1(q)\exp[-\Gamma_1(q)\,t] + a_2(q)\exp[-\Gamma_2(q)\,t]$. The relaxation frequency, or the decay rate, $\Gamma_1(q)$, for the slow mode of motion gave the translational diffusion coefficient of the entire copolymer molecule at $q \to 0$ and $c \to 0$ (the long-time diffusion coefficient). The diffusive motion, however, is retarded by the influence of the strong intrachain hydrodynamic interactions; the diffusion motion couples very strongly with the internal modes of motion and the coupling deforms the block copolymer chain during diffusion. The unexpected small fractional amplitude of the diffusion motion, a_1, confirms also the vast hydrodynamic interactions taking place in the diblock chain in solution. On the other hand, the decay rate for the fast mode of motion, $\Gamma_2(q)$, gives information on the internal motions which appear peculiarly in the diblock copolymer and are called the copolymer mode: In the small q limit, a constant $(\Gamma_2)_{c\to0,q\to0}$, which has been predicted theoretically, was not detected and a diffusion-like term $[(\Gamma_2-\Gamma_1)/q^2]_{c\to0,q\to0}$ was observed instead, indicating a motion about 2 times faster than the entire diblock chain diffusion. With an increase of q, the Γ_2 increased and showed the q^3 dependence which is characteristic of chains with nondraining hydrodynamic interactions. Further, this q^3 dependence is reached at a remarkably small value of qR_G as compared with flexible linear chains in good solvents. This feature was attributed to the vast dynamical heterocontact effect, or hydrodynamic interactions between the PS and the PMMA subchain elements. The strong hydrodynamic interactions were also discussed in terms of the first cumulant which mediates the short-time behavior of the block chain. Finally, the dynamical intermolecular interaction was examined through the concentration dependence of the diffusion coefficient k_D^V. The result shows that the k_D^V of the diblock chain can be well represented by the Akcasu–Benmouna formula which also holds good for flexible linear polymers in good solvents.

Introduction

The dynamic behavior of flexible linear homopolymers in dilute solutions has been extensively investigated by dynamic light scattering (DLS). In this case, the translational diffusion motion observed at $qR_G \ll 1$ represents distinctly the center-of-mass diffusion of a single polymer chain. The faster modes of motion, appearing with increase of qR_G, contain information on the intramolecular (internal) relaxation motions of the chain. These DLS results, connected with theoretical works, have been effective in understanding precisely polymer chain dynamics in solution.[1,2] Here q and R_G denote the magnitude of the scattering vector and the root-mean-square radius of gyration of the polymer, respectively.

For flexible diblock copolymer chains of type AB, on the other hand, the situation becomes complicated even in the case of dilute solutions. The diffusion coefficient and the internal modes of motion are affected by the hydrodynamic interactions operating not only in the individual subchain A or B but also in the pair of subchains A and B. In the presence of such hydrodynamic interactions, it has been indicated theoretically[3–6] that the external center-of-mass motion and the internal motions of the chain are in general coupled, and the coupling leads to deformation of the chain during diffusion; the intrachain segmental distribution about the center of mass deviates from its spherical equilibrium distribution. The coupling thus induces a difference in the relaxation times of the external and internal motions of the entire chain and leads to a distinction between the short-time and long-time diffusion coefficients, D and D_{sh}, respectively. The correction term $\Delta = D_{sh} - D$ has been predicted to produce an error of 15% (Zimm) or errors on the order of a few percent (Fixman) even in homopolymers with a nonpreaveraged Oseen tensor.[3] For the AB diblock copolymer solutions, special attention should be required because the relative motion of the A and B parts involves the internal modes of the entire copolymer chain and cannot be treated in the Markoff limit where the long-time behavior ($q \to 0$ and $t \to \infty$ with q^2t constant) is being considered.[5] Thus, even if we deal only with a component subchain, e.g., subchain A, the subchain will show in dilute solutions different dynamical behavior from that for the homopolymer chain A whose molecular weight is exactly the same as that of subchain A.

When an attempt is made by DLS to examine the dynamic behavior of such diblock chains in solutions, it will be difficult to interpret because the translational diffusion and the internal modes of motion couple with each other[3–6] and the apparent values that can be obtained depend strongly on the refractive index differences between subchains A and B and the solvent used.[7] However, if subchain B is made invisible optically by choosing a solvent matching the refractive index of the B part,[8] the dynamical behavior of subchain A in the diblock copolymer can be made clear.

Under the condition mentioned above, the observed dynamic structure factor of the AB diblock copolymer,

0024-9297/93/2226-4899$04.00/0

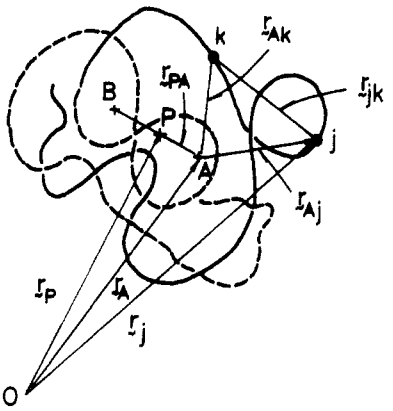

Figure 1. Sketch of an AB diblock copolymer chain in a refractive-index-matched solvent. The solid line represents the visible subchain A and the broken line the invisible subchain B. Positions P, A, and B represent the center of masses of the AB diblock chain and subchains A and B, respectively.

$S(q,t)$, will describe the light scattered only from subchain A and is expressed by

$$S(q,t) = (M/p_A)^2 \sum_j \sum_k \langle \exp[i\mathbf{q}\cdot\mathbf{r}_{jk}(t)] \rangle \qquad (1)$$

with M the molecular weight of the block chain and p_A the number of monomeric units of subchain A. Here $\mathbf{r}_{jk}(t)$ is the time-dependent distance between elements j and k at positions $\mathbf{r}_j$ and $\mathbf{r}_k$ of the A part, respectively, i.e., $\mathbf{r}_{jk} = \mathbf{r}_j(0) - \mathbf{r}_k(t)$. As shown in Figure 1, where the visible part A (the solid line) and the invisible part B (the broken line) are penetrating each other, the position $\mathbf{r}_j$ in subchain A can be given by $\mathbf{r}_j = \mathbf{r}_P + \mathbf{r}_{PA} + \mathbf{r}_{Aj}$ with $\mathbf{r}_P$ the center-of-mass position of the entire block chain, $\mathbf{r}_{PA}$ the distance between the center of masses of the block and subchain A, and $\mathbf{r}_{Aj}$ the distance of the j element from the center of mass of subchain A. If $\mathbf{r}_P$, $\mathbf{r}_{PA}$, and $\mathbf{r}_{jk}$ were uncorrelated with each other and the intramolecular interactions of subchain A with subchain B were neglected, $S(q,t)$ might be broken down into three contributions due to the motion of the center-of-mass position $\mathbf{r}_P$, the fluctuation of the relative center-of-mass distance between the A and B subchains, $\mathbf{r}_{AB}$, and the distance fluctuation within subchain A, $\mathbf{r}_{jk}$;

$$S(q,t) \propto \langle \sum_P \exp\{i\mathbf{q}\cdot[\mathbf{r}_P(0)-\mathbf{r}_P(t)]\} \sum_A \exp\{i\mathbf{q}\cdot [\mathbf{r}_{PA}(0)-\mathbf{r}_{PA}(t)]\} \sum_j \sum_k \exp\{i\mathbf{q}\cdot[\mathbf{r}_{Aj}(0)-\mathbf{r}_{Ak}(t)]\} \rangle \qquad (2)$$

In this situation, eq 2 predicts that (1) the center-of-mass diffusion of subchain A, not of the entire block chain, will be observed in the short-time limit of $q \to 0$ and $t \to 0$ since the first two terms on the right-hand side of eq 2 can be reduced to the motion of the center-of-mass position of the A part, r_A and that (2) with an increase of qR_G, the internal modes of motion characteristic of the elements in subchain A, as well as the diffusion of the A part relative to the B part, will become dominant and detectable. As pointed out by Akcasu et al.[3-6] and already described, however, these motions are correlated with each other and the observed modes of motions in DLS experiments are, in general, not related directly to the diffusion coefficients characterizing the so-called cooperative diffusion and interdiffusion processes, the former mediating the relaxation of the total number of density fluctuations of the pair of subchains A and B and the latter the relaxation of thermal fluctuations in the relative local concentrations of a pair of subchains A and B toward their equilibrium values, respectively.

Table I. Thermodynamic Characteristics of a Polystyrene–Poly(methyl methacrylate) Diblock Copolymer, BMM313, Its Precursor Polystyrene, RS-13, and Benzene at 30 °C and/or at 488 nm

polymer code	styrene content, wt %	$M_w \times 10^{-6}$	$A_2 \times 10^4$, mol cm^3 g^{-2}	$A_3 \times 10^{12}$, mol cm^6 g^{-3}	R_G, nm
BMM313[a]	38.5	1.53	1.67	−1.12[b]	41.0
RS-13[a]	100	0.589	3.56		36.2

		dn/dc, cm^3 g^{-1}		
solvent	n_0	PS	PMMA	BMM313
benzene	1.5060	0.1105	0.0003	0.0427

[a] Prepared by anionic polymerization. [b] The concentration range was 0–5.39 × 10^{-3} g cm^{-3}.

In this paper, we aim to investigate the details of such dynamical modes of motion in an AB-type diblock copolymer in dilute solution. In order to attain this aim, we chose as the copolymer sample a polystyrene-poly(methyl methacrylate) (PS–PMMA) diblock copolymer of relatively high molecular weight and used benzene as the solvent. The high-molecular-weight sample makes it easy to detect the internal motions in the subchain. Benzene is a good solvent for both PS and PMMA and is isorefractive to PMMA at 30.0 °C for light of 488 nm. DLS experiments were carried out at 30 °C by a 488-nm line of an etalon-equipped argon-ion laser. Six dilute solutions ranging from 0.122c^* to 0.657c^* were measured at scattering angles in the range 10–150°, with c^* the overlapping polymer concentration. For references, a PS homopolymer of molecular weight exactly the same as that of subchain A was also examined, the homo-PS being a precursor of the anionic polymerization of the present PS–PMMA sample.

Experimental Section

Materials. A PS–PMMA diblock copolymer sample, used in the present study and coded as BMM313, was prepared by anionic polymerization at −78 °C under 10^{-6} mmHg with *sec*-butyllithium as the initiator and tetrahydrofuran (THF) as the solvent; the PS part was prepared first, and then the PMMA part followed.[9] The homo-PS, separated and terminated just before performing the PMMA polymerization, had thus a molecular weight identical with that of the PS subchain in BMM313. The homo-PS was designated as RS-13. These samples were characterized by static light scattering in benzene at 30.0 °C[9] and by GPC in THF at 40 °C[10] with the results that the weight-average molecular weight $M_w = 1.53 \times 10^6$, $M_w/M_n = 1.01$, the PS content = 38.5 wt %, and the $R_G = 41.0_2$ nm for the block copolymer, BMM313, and $M_w = 0.589 \times 10^6$, $M_w/M_n = 1.01$, R_G(homo) = 36.2 nm for the homo-PS, RS-13.[10] These values are listed in Table I. Polymer solutions of given concentrations ($c < c^*$) were first prepared by dissolving the copolymer sample in spectrograde benzene at room temperature and were left overnight at ca. 40 °C. Six sample solutions were then prepared by mixing the original solution with solvent, the solution and the solvent being filtered through 0.5- and 0.2-μm Millipore filters, respectively, into dust-free light scattering cells, and were left for more than 1 week at 30 °C prior to measurement.

The overlapping polymer concentration c^* was calculated to be 2.44 × 10^{-3} g cm^{-3} by using the relation $c^* \simeq [\eta]^{-1}$. The intrinsic viscosity $[\eta]$ of BMM313 in benzene was measured at 30.00 ± 0.02 °C with an Ubbelohde capillary viscometer. The result gave $[\eta]$ = 410 cm^3 g^{-1} and the Huggins constant k' = 0.332. For RS-13, $[\eta]$ = 184 cm^3 g^{-1} and k' = 0.340 in benzene at 30.00 °C. Isorefractivity of the solvent, benzene, to PMMA for the 488-nm line at 30 °C was ascertained, as shown in Table I, by refractometry and static and dynamic light scattering measurements for benzene solutions of a homo-PMMA sample; the PMMA sample was prepared also by anionic polymerization[11] and its molecular weight, $M_w = 1.10 \times 10^6$, was nearly the same as that of the PMMA subchain of the present block copolymer, $M_w = 0.941 \times$

10^6. The PMMA-benzene solutions did not exhibit any detectable decay in their time correlation functions for 488 nm at 30 °C over the whole range of polymer concentration and of scattering angle measured.

Dynamic Light Scattering and Data Analyses. The normalized homodyne time correlation function $A(t)$ of the vertically-polarized-light intensity scattered by a vertically-polarized 488-nm line of an etalon-equipped 3-W argon-ion laser (Spectra Physics, 2020/2560) was measured with our laboratory-made time-interval software correlator (512 channels)[12] at scattering angles in the range 10–150° at 30.00 ± 0.02 °C. In each measurement, $A(t)$ data were accumulated for more than 1 h under the laser light intensity stabilized to within ±0.5% fluctuation. The accuracy of each data point was guaranteed to within 2–3%, and the base-line value was strictly checked to be 1.000 ± 0.003, i.e., $\delta = \pm 0.003$ in the following relation between $A(t)$ and the normalized scattered-field correlation function, $g^{(1)}(t)$,

$$A(t) = \beta|g^{(1)}(t)|^2 + 1 + \delta \tag{3}$$

where β is the spatial coherence factor depending on the detection geometry.

The inverse Laplace transformation of $A(t)$, or the $A(t)$ profile analysis, was performed through the histogram method operating on a weighted nonlinear least-squares algorithm with a FACOM M-760/10 computer in our institute.[13] The distribution $G(\Gamma)$ of the characteristic decay rate Γ for $g^{(1)}(t)$ was expressed by multimode histograms extending over a region in Γ space, the histograms in mode i being represented by a number of equally segmented histogram steps m_i, the width of each step $\Delta\Gamma_i$, and the height of the jth step H_{ij}. The function $g^{(1)}(t)$ is thus given by

$$g^{(1)}(t) = \int_0^\infty G(\Gamma) \exp(-\Gamma t)\, d\Gamma \tag{4}$$

The mean decay rate Γ_i and the fractional amplitude a_i for mode i are related to the first cumulant Γ_e as $\Gamma_e = \int_0^\infty \Gamma G(\Gamma)\, d\Gamma = \sum_i a_i\Gamma_i$ with $\Gamma_i = (1/a_i)\sum_{j=1}^{m_i} \Gamma_{ij}H_{ij}\Delta\Gamma_i$, $a_i = \sum_{j=1}^{m_i} H_{ij}\Delta\Gamma_i$, and $\sum_{i=1}^{m} a_i = 1$ (the normalization condition). Here m represents the number of modes of motion existing in the solution under consideration. In bimodal histograms, or $m = 2$, the Γ_e of the whole histogram was evaluated as

$$\Gamma_e = \int_0^\infty \Gamma G(\Gamma)\, d\Gamma = a_1\Gamma_1 + a_2\Gamma_2 \tag{5}$$

with

$$\Gamma_e \equiv -\lim_{t\to 0} (d|g^{(1)}(t)|/dt) \tag{6}$$

When subchain B of the AB diblock copolymer is made invisible, the bimodal, or the two-exponential mode expression for $g^{(1)}(t)$

$$|g^{(1)}(t)| \equiv S_A(q,t)/S_A(q)$$
$$= a_1(q) \exp[-\Gamma_1(q)t] + a_2(q) \exp[-\Gamma_2(q)t] \quad (\Gamma_1 < \Gamma_2) \tag{7}$$

will be convenient, as a starting point, to analyze the $A(t)$ of the visible part A. Here $S_A(q,t)$ and $S_A(q)$ are the dynamic and static structure factors of the visible A part, respectively, and we denote the slower decay mode as mode 1; $\Gamma_1 < \Gamma_2$. The expression of eq 7 was obtained first by Akcasu et al.[6] by using the theory of binary polymer solutions and treating the A and B subchains of the copolymer as two different components. According to a very recent study on a single diblock copolymer in the free-draining hydrodynamic-interaction (Rouse) limit, Akcasu[5] has shown that the slow mode $\Gamma_1(q)/q^2$ approaches the long-time diffusion coefficient of the entire copolymer molecule D_{copol} as $q \to 0$, which is defined in terms of the mean-square displacement of the center of mass of the whole molecule at $t \to \infty$. On the other hand, the fast mode Γ_2 approaches a constant,[5] which corresponds to the copolymer mode. The first cumulant Γ_e follows from eq 7 as

$$\Gamma_e(q) = a_1(q)\,\Gamma_1(q) + a_2(q)\,\Gamma_2(q) \tag{8}$$

and in the small q limit $\Gamma_e(q)/q^2$ approaches the diffusion coefficient of the subchain, $D_A = D_{homo\text{-}A}$; $g^{(1)}(t)$ is in this case expressed as

$$|g^{(1)}(t)| = a_1(q) \exp(-D_A q^2 t) + a_2(q) \exp[-(D_A q^2 + 2\tau_c^{-1})t] \tag{9}$$

with the collective internal relaxation time τ_c as

$$2\tau_c^{-1} = \Gamma_2(q) - \Gamma_1(q) \tag{10}$$

At infinite dilution $c \to 0$, it is obtained that

$$D(c=0) = D_{0,homo\text{-}A}, \quad (a_1)_{c\to 0} \equiv a_1(q,c=0) \tag{11}$$

where $D_{0,homo\text{-}A}$ is the translational diffusion coefficient of the A part and $(a_1)_{c\to 0}$ is the fractional amplitude of the diffusion motion. Therefore, in the data analyses, the q dependence of Γ_1/q^2, Γ_e/q^2, and Γ_2 (or $\Gamma_2 - \Gamma_1$), and their limiting behavior at $q \to 0$ and $c \to 0$ are examined basically.

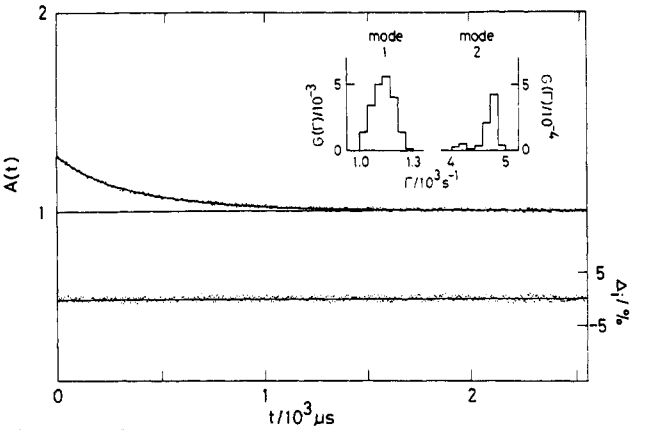

Figure 2. Time correlation function $A(t)$ and the fitting error $\Delta_i(\%)$ plotted against time t for a PS-PMMA diblock copolymer in benzene at 30 °C: polymer mass concentration $c = 0.390_4 \times 10^{-3}$ g cm^{-3} and scattering angle $\theta = 30°$. Inset: the two-mode-type histogram $G(\Gamma)$ for $|g^{(1)}(t)|$ plotted against the decay rate Γ. The dots denote 511 data points, and the solid curve $A(t)$ represents the fitting curve obtained by the histogram $G(\Gamma)$.

Results and Discussion

Existence of Two Modes of Motion. The time correlation functions for six BMM313-benzene solutions of polymer mass concentration, 10^3c (g cm^{-3}) = 0.296_9, 0.390_4, 0.494_6, 0.541_3, 1.10_4, and 1.60_2, were measured at six scattering angles 10°, 30°, 60°, 90°, 120°, and 150°, the angles covering the $(qR_G)^2$ range of 0.0192–2.53. As expected in the previous section, all the $A(t)$ functions measured were not expressed by curves of single-exponential decay; i.e., $|g^{(1)}(t)|$ in eq 4 was not represented by a one-mode Γ distribution but by curves for a two-mode Γ distribution where each Γ was separated distinctly. A typical correlation function and its resultant $G(\Gamma)$ distribution for $|g^{(1)}(t)|$ are illustrated in Figure 2 for a solution of $c = 0.390_4 \times 10^{-3}$ g cm^{-3} and scattering angle $\theta = 30°$. This result shows that the dynamics in the present system are characterized by at least two modes of motion. We denote the slow mode as mode 1, represented by the smaller mean decay rate Γ_1, and the fast mode as mode 2, with $\Gamma_2 > \Gamma_1$. Table II summarizes as functions of θ and c the decay rates, $\Gamma_1(q,c)$ and $\Gamma_2(q,c)$, and the first cumulant, $\Gamma_e(q,c)$, for all the solutions measured. Here q is given by $q = (4\pi n_0/\lambda_0)\sin(\theta/2)$ with λ_0 the wavelength of the incident light in vacuum and n_0 the refractive index of benzene at 30 °C and at 488 nm (Table I).

Figure 3 gives a broad outline of the q and c dependence of the mean decay rate Γ_i for the two modes of motion, where Γ_i/q^2 for mode 1 ($i = 1$) and mode 2 ($i = 2$) at two selected angles, $\theta = 30°$ and 120°, is plotted against c on a logarithmic scale. Since the behavior at $\theta = 30°$ and 120° represents typically the chain dynamics at $(qR_G)^2 \ll 1$ and at $(qR_G)^2 > 1$, respectively, these plots show that

Table II. Mean Decay Rates of Modes 1 and 2, Γ_1 and Γ_2, the First Cumulant, Γ_e, and the Fractional Amplitude of Mode 1, a_1, for PS-PMMA Diblock Copolymer, BMM313, in Benzene at 30 °C (Γ_i/q^2 and Γ_e/q^2 Given in Units of 10^{-7} cm^2 s^{-1} and Γ_i in Units of s^{-1})

	$\theta = 10°$, $q^2 = 0.0114_2 \times 10^{11}$ cm^2	$\theta = 30°$, $q^2 = 0.100_8 \times 10^{11}$ cm^2	$\theta = 60°$, $q^2 = 0.376_0 \times 10^{11}$ cm^2	$\theta = 90°$, $q^2 = 0.752_0 \times 10^{11}$ cm^2	$\theta = 120°$, $q^2 = 1.12_8 \times 10^{11}$ cm^2	$\theta = 150°$, $q^2 = 1.40_8 \times 10^{11}$ cm^2	$\theta \to 0$, $q \to 0$
			$c = 0.296_9 \times 10^{-3}$ g cm^{-3}				
Γ_1/q^2	1.16	1.14	1.16	1.17	1.16	1.16	1.16
Γ_2/q^2	3.96	4.55	5.50	6.07	7.40	7.02	
Γ_e/q^2	1.20	1.28	1.57	1.92	2.54	2.75	
a_1	0.98	0.96	0.88	0.85	0.80	0.76	
			$c = 0.390_4 \times 10^{-3}$ g cm^{-3}				
Γ_1/q^2	1.18	1.19	1.17	1.17	1.18	1.18	1.18
Γ_2/q^2	3.81	4.63	5.58	6.20	7.41	7.16	
Γ_e/q^2	1.21	1.32	1.61	1.91	2.53	2.68	
a_1	0.98	0.95	0.87	0.84	0.80	0.75	
			$c = 0.494_6 \times 10^{-3}$ g cm^{-3}				
Γ_1/q^2	1.21		1.20	1.20	1.19	1.20	1.20
Γ_2/q^2	4.17		5.36	6.04	7.53	7.19	
Γ_e/q^2	1.26		1.62	1.91	2.52	2.59	
a_1	0.98		0.86	0.81	0.80	0.76	
			$c = 0.541_3 \times 10^{-3}$ g cm^{-3}				
Γ_1/q^2	1.20	1.20	1.19	1.20	1.22	1.21	1.21
Γ_2/q^2	4.07	4.65	5.47	6.11	7.32	7.05	
Γ_e/q^2	1.25	1.36	1.65	1.91	2.50	2.60	
a_1	0.97	0.94	0.86	0.83	0.80	0.75	
			$c = 1.10_4 \times 10^{-3}$ g cm^{-3}				
Γ_1/q^2	1.28	1.27	1.27	1.27	1.29	1.29	1.28
Γ_2/q^2	4.04	4.66	5.45	6.21	7.57	6.59	
Γ_e/q^2	1.41	1.54	1.74	1.91	2.32	2.34	
a_1	0.97	0.93	0.87	0.86	0.84	0.80	
			$c = 1.60_2 \times 10^{-3}$ g cm^{-3}				
Γ_1/q^2	1.32	1.32	1.32	1.36	1.34	1.32	1.33
Γ_2/q^2	4.05	4.74	4.82	5.82	6.91	6.47	
Γ_e/q^2	1.50	1.66	1.83	1.89	2.21	2.20	
a_1	0.96	0.94	0.85	0.81	0.85	0.81	
			$c \to 0$ g cm^{-3}				
Γ_1/q^2							1.13
Γ_2/q^2	4.04	4.65	5.47	6.11	7.41	7.10	(3.65)
$(\Gamma_2-\Gamma_1)/q^2$	2.80	3.43	4.27	4.92	6.24	5.91	(2.50)
Γ_e/q^2	1.13	1.21	1.53	1.92	2.64	2.83	1.13
a_1	0.99	0.96	0.87	0.84	0.78	0.74	
Γ_2	462	4680	20570	45930	83650	99630	
$\Gamma_2-\Gamma_1$	320	3450	16070	37010	70370	82970	

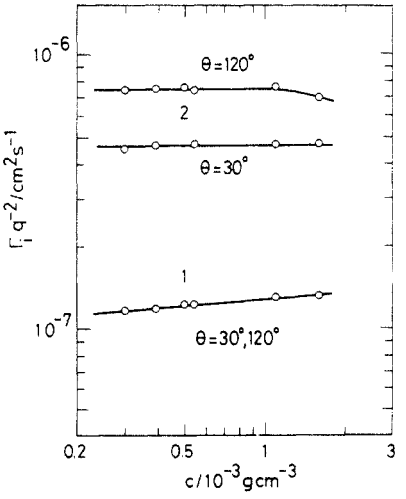

Figure 3. Broad outline of the q and c dependence of the mean decay rate Γ_i for the two modes of motion, $i = 1$ and 2, of PS-PMMA diblock copolymer in benzene at 30 °C. The Γ_i/q^2 behavior at $qR_G \ll 1$ and $qR_G > 1$ is represented by the curves at the scattering angles $\theta = 30°$ and 120°, respectively.

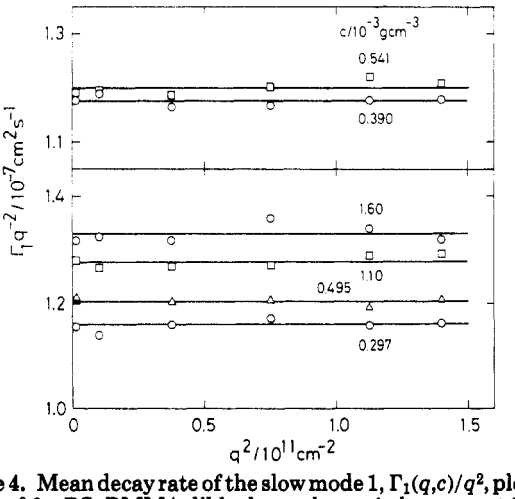

Figure 4. Mean decay rate of the slow mode 1, $\Gamma_1(q,c)/q^2$, plotted against q^2 for PS-PMMA diblock copolymer in benzene at 30 °C at six polymer mass concentrations c ranging from 0.297×10^{-3} to 1.60×10^{-3} g cm^{-3}.

Γ_1/q^2 is independent of q, but Γ_2/q^2 is not. In addition, the plots indicate that both Γ_1/q^2 and Γ_2/q^2 are linear in c in the region of small c. In what follows, we discuss the behavior of these modes of motion in more detail.

Slow Mode. Figure 4 shows plots of $\Gamma_1(q,c)/q^2$ versus q^2 for six different values of c. The Γ_1/q^2 is constant, independent of q at a given c. This behavior is characteristic of the translational diffusion motion. We therefore determined the diffusion coefficient, $D(c)$, from the $(\Gamma_1/q^2)_{q\to 0}$ values, which were estimated as the average of six $\Gamma_1(q,c)/q^2$ values at different scattering angles. The $D(c)$ values thus obtained are plotted against c in Figure 5. Six data points are represented well by the equation

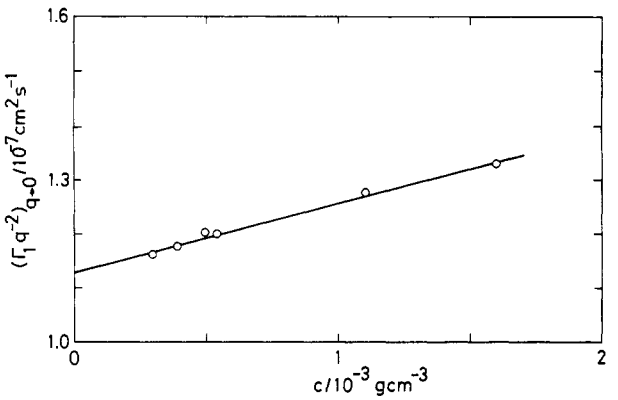

Figure 5. Concentration dependence of the mean decay rate of the slow mode at $q \to 0$, $(\Gamma_1/q^2)_{q\to 0}$, which is the translational diffusion coefficient at finite c, $D(c)$, for PS–PMMA diblock copolymer in benzene at 30 °C.

$$D(c) = D_0(1 + k_D c) \tag{12}$$

and yield the translational diffusion coefficient at infinite dilution, $D_{0,\text{block}}$, and the concentration coefficient, k_D, as 1.13×10^{-7} cm^2 s^{-1} and 113 cm^3 g^{-1}, respectively. The Stokes–Einstein equation, $D_0 = k_B T/6\pi\eta_s R_H$, gave the hydrodynamic (Stokes) radius, R_H, as $R_{H,\text{block}} = 35.0$ nm. Here k_B represents Boltzmann's constant and η_s the bulk solvent viscosity, η_s(benzene,30°C) $= 5.621 \times 10^{-3}$ g cm^{-1} s^{-1}.

On the other hand, DLS measurements for homo-PS, RS-13, were made for five solutions of $0.392_1 \times 10^{-3}$–$2.00_3 \times 10^{-3}$ g cm^{-3} at $\theta = 10°$, 30°, and 60° where $(qR_G)^2 < 1$. All the correlation functions measured showed single-exponential types of decays and gave the diffusion coefficient $D_{0,\text{homo}} = 1.59 \times 10^{-7}$ cm^2 s^{-1}, or $R_{H,\text{homo}} = 24.8$ nm, and the concentration coefficient $k_{D,\text{homo}} = 118$ cm^3 g^{-1}. Table III summarizes the results thus obtained for BMM313 and RS-13.

In the third row in Table III, the ratio of R_G for the block copolymer (BMM313) to that for homo-PS (RS-13), $R_{G,\text{block}}/R_{G,\text{homo}}$, is shown to be 1.13, which is considerably larger than unity. The large R_G ratio reflects that there is heterocontact thermodynamic interaction between the intramolecular PS and PMMA elements. This thermodynamic interaction makes the PS–PS segment distances larger than those in the homo-PS; the visible PS and invisible PMMA subchains interpenetrate each other in a more stretched state than in the case of the homopolymers. This situation prevents intramolecular separation (segregation) of the PS and PMMA subchains,[14] because the segregation leads to a rough equality for the visible PS part as $R_{G,\text{block}} \simeq R_{G,\text{homo}}$.

In the present case where the PS and PMMA parts interpenetrate each other and are considered to mix uniformly as a single-block chain in the sense of long-time behavior, the visible radius of gyration, $R_{G,\text{block}} = 41.0$ nm (Table III), represents roughly the overall radius of gyration of the block chain. The corresponding hydrodynamic radius $R_{H,\text{block}}$ or the diffusion coefficient $D_{0,\text{block}}$ is not equal to the diffusion coefficient $D_{0,\text{homo}}$ of the homo-PS part (the short-time diffusion coefficient) but is equal to the center-of-mass diffusion coefficient $D_{0,\text{copol}}$ of the entire copolymer chain, i.e., the long-time diffusion coefficient.[3,5] The reason is that for the short times the diffusion of the PS part does not feel the effect of the invisible PMMA part, but after long times the effect works and the PS and PMMA parts diffuse together. Therefore, it is suitable to compare the experimental $D_{0,\text{block}}$ to the entire-chain value $D_{0,\text{copol}}$.

Concerning the entire copolymer chain, not just the PS part, we consider a hypothetical PS chain which has the total number of monomers p equal to that of the whole block copolymer BMM313, i.e., $p = p_S + p_{PMMA} = M_{PS}/m_{PS} + M_{PMMA}/m_{PMMA}$ with p_S and m_{PS} the total number of monomers and the monomer mass of the PS part, respectively. The molecular weight that results is $M_{w,\text{hypo}} = 1.568 \times 10^6$. For the hypothetical PS, its characteristic values were calculated to be $R_{H,\text{hypo}} = 40.9$ nm and $R_{G,\text{hypo}} = 59.6$ nm by using the reference relations in benzene at 30 °C ($R_H = 1.60 \times 10^{-9} M_w^{0.55}$ and $R_G^2 = 2.31 \times 10^{-18} M_w^{1.16}$),[15-17] as are shown in the fourth column of Table III. If the visible PS subchain in the block copolymer suffers the same hydrodynamic interactions as was observed in the nondraining homopolymer chains, the corresponding Stokes radius will obey the relation $R_G/R_H \simeq 1.50$, which has empirically been established for linear flexible chains in good solvents[15,18] and is typically exemplified by homo-PS (RS-13) in Table III ($(R_G/R_H)_{\text{homo}} = 1.46$). However, the experimental value for the visible PS, $R_{H,\text{block}} = 35.0$ nm, is beyond this expectation, as is shown in the ratio $R_{G,\text{block}}/R_{H,\text{block}} = 1.17$ (Table III), which is much smaller than 1.46. Akcasu[5] has indicated that in Rouse dynamics, where the hydrodynamic interactions are absent, the center-of-mass diffusion of the block chain and the internal modes are uncoupled, and the translational diffusion coefficient $D_{0,\text{copol}}$ can be given by

$$D_{0,\text{copol}}^{-1} = D_{0,\text{homo-A}}^{-1} + D_{0,\text{homo-B}}^{-1} \tag{13a}$$

or

$$R_{H,\text{copol}} = R_{H,\text{homo-A}} + R_{H,\text{homo-B}} \tag{13b}$$

where $D_{0,\text{homo-A}}$ is the translational diffusion coefficient of subchain A and takes the same value in both cases of short-time and long-time behaviors. In the present experiments, the R_H value for the PS part $R_{H,\text{homo-PS}}$ (=24.8 nm; Table III) was obtained, but not for the PMMA part because the PMMA is invisible in benzene. If we substitute the PMMA part with PS of the same number of monomers as the PMMA part, as treated above, we may estimate $R_{H,\text{homo-PMMA}}$ by using refs 15 and 17 as $R_{H,\text{homo-PMMA}} = 31.6$ nm. Substitution of these R_H values into eq 13 gives $R_{H,\text{copol}} = 56.4$ nm. This value again is beyond the experimental one, $R_{H,\text{block}} = 35.0$ nm. These circumstances mean that the center-of-mass diffusion of the block chain suffers significantly strong intrachain hydrodynamic interactions in the course of its diffusion. In other words, the diffusive

Table III. Dynamic Characteristics of PS–PMMA Diblock Copolymer, BMM313, and Homo-PS, RS-13, in Benzene at 30 °C

polymer	R_G, nm	D_0, 10^{-7} cm^2 s^{-1}	R_H, nm	R_G/R_H	k_D, cm^3 g^{-1}	$[\eta]$,[a] cm^3 g^{-1}	R_V,[a] nm
block PS part (BMM313)	41.0	1.13	35.0	1.17	113	410	46.3
homo-PS (RS-13)	36.2	1.59	24.8	1.46	118	184	25.8
$R_{\text{block}}/R_{\text{homo}}$	1.13	$(1.41)^{-1}$	1.41				
		Hypothetical Values					
hypothetical PS ($p = p_{PS}+p_{PMMA}$)[b]	59.6[c]	0.966[d]	40.9[d]	1.46		365[c]	44.9
$R_{\text{block}}/R_{\text{PS,hypo}}$	0.688	$(0.855)^{-1}$	0.855				1.03

[a] The viscometric radius R_V is defined with the intrinsic viscosity $[\eta]$ as $R_V = [(3/4\pi)(2/5N_A)]^{1/3}(M_w[\eta])^{1/3}$. Here N_A is Avogadro's constant. [b] p denotes the number of monomeric units of the block chain, p_{PS} and p_{PMMA} being that in the PS and PMMA subchains, respectively. [c] Reference 16. [d] References 15 and 17.

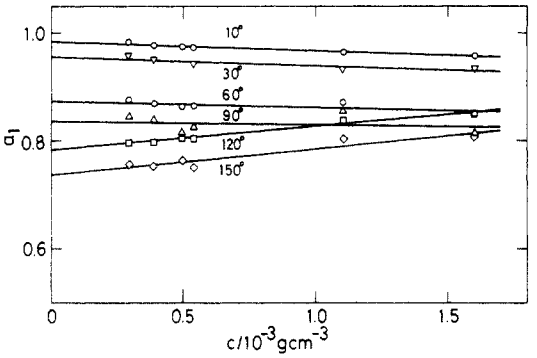

Figure 6. Concentration dependence of the fractional amplitude of the slow mode $a_1(c)$ for the PS–PMMA diblock copolymer in benzene at 30 °C at six scattering angles ranging from 10° to 150°.

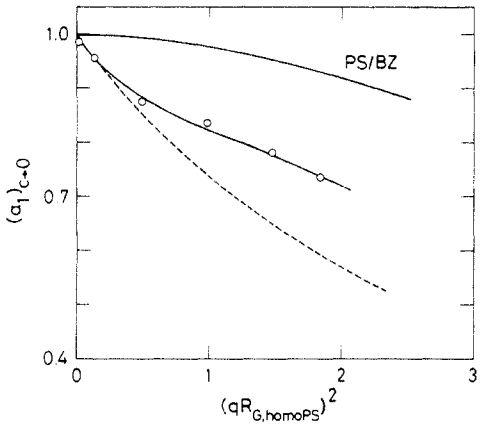

Figure 7. Fractional amplitude of the slow mode at infinite dilution, $(a_1)_{c\to 0}$, plotted against $(qR_{G,homo\text{-}PS})^2$: (O) the present data for the PS–PMMA diblock copolymer in benzene at 30 °C. The broken curve represents the theoretical prediction for a labeled diblock copolymer in Rouse dynamics,[5] where the PS part is labeled. The visible part is PS. The solid curve PS/BZ represents our previous data for PS in benzene at 30 °C.[15]

motion of the diblock molecule couples very strongly with the internal modes of motion in solution.

Fractional Amplitude of the Diffusion Mode. Figure 6 shows the concentration dependence of the fractional amplitude of the slow mode, $a_1(q,c)$ in eq 7, at constant q. The data for each q depend linearly on c, as shown by the solid lines in the figure, from which the infinite dilution values, $(a_1)_{c\to 0}$, were estimated. The slopes increase, changing sign from negative to positive, with increasing q. The increase in slope is in agreement with previous experimental data for homopolymers in good solvents.[15,18] In Figure 7, the $(a_1)_{c\to 0}$ at given q is plotted against $(qR_{G,homo\text{-}PS})^2$ by unfilled circles where $R_{G,homo\text{-}PS}$ denotes the mean-square radius of gyration of PS chains. In the same figure, the empirical $(a_1)_{c\to 0}$ values obtained previously for linear PS chains in benzene at 30 °C[15] are also shown by a solid curve PS/BZ. From the figure, the amplitude of the diffusive motion for the present block chain is found to be much smaller than in the case of PS chains. This means that nondiffusional motions are vigorous in the block chain. The internal modes of motion originating purely from the homo-PS chain are not sufficient in magnitude to account for such a large amount of nondiffusional motion as shown in Figure 7. Other intramolecular modes of motion are needed to explain this behavior.

Theoretically the amplitudes a_1 and a_2 of $|g^{(1)}(t)|$ in eq 7 are predicted in Rouse dynamics as[5]

$$a_1(q) = [\Gamma_2(q) - \Gamma_1(q)]^{-1}[\Gamma_2(q) - q^2k_BT\mu_A(q)/S_A(q)] \quad (14a)$$

$$a_2(q) = [\Gamma_1(q) - \Gamma_2(q)]^{-1}[\Gamma_1(q) - q^2k_BT\mu_A(q)/S_A(q)] \quad (14b)$$

where $S_A(q)$ and $\mu_A(q)$ are the static structure factor and the mobility of the visible part A, respectively. It should be noted here that the difference between the short-time and long-time behaviors disappears in Rouse dynamics. In the limit as $q \to 0$, $\Gamma_1(q)$ and $\Gamma_2(q)$ in eq 14 approach[5]

$$\Gamma_1(q\to 0) = D_{0,copol}q^2 \quad (15a)$$

$$\Gamma_2(q\to 0) = (3/2)(D_{0,homo\text{-}A} + D_{0,homo\text{-}B})/(R_{GA}^2 + R_{GB}^2) \quad (15b)$$

where $D_{0,copol}$ is given by eq 13. As $q \to 0$, $\Gamma_2(q)$ remains constant, whereas $\Gamma_1(q)$ vanishes. Therefore, from eq 14, the amplitude $a_2(q)$ of the fast mode vanishes at all times as $q \to 0$ and the amplitude $a_1(q)$ in the small q limit becomes the particle scattering factor of the visible A part, $P_A(q)$;

$$a_1(q) = P_A(q) \quad (16)$$

and eq 7 reduces to[5]

$$|g^{(1)}(t)| = P_A(q)\exp(-D_{0,copol}q^2)t \quad (17)$$

which is the single-exponential-decay function representing the center-of-mass diffusion of the entire copolymer chain, as already described. $P_A(q)$ will be conventionally expressed by the Debye function for Gaussian chains

$$P_D(x_A) = (2/x_A^2)[\exp(-x_A) - 1 + x_A) \quad (18)$$

with $x_A = (qR_{GA})^2$, but it has been recognized experimentally[19] that the P_D expression holds well even in good solvents up to $x \simeq 10$. The broken curve in Figure 7 represents this prediction, $a_1(q) = P_D(x_{homo\text{-}PS})$, where the hydrodynamic interactions are absent. The curve is located well below the experimental data. This deviation indicates again the strong hydrodynamic interactions acting upon the monomers in the diblock copolymer chain. Unfortunately, there is no theoretical prediction of $a_1(q)$ which takes into account of the hydrodynamic interactions, because $a_1(q)$ in this case will not represent a purely uncoupled amplitude of the diffusion motion but will include complex effects coming from the coupling between the diffusion and the internal modes of motion.

Fast Mode. As already shown roughly in Figure 3, the mean decay rate of the fast mode, i.e., $\Gamma_2(q,c)/q^2$, has a strong q and c dependence. The detailed behavior of this mode is shown in Figure 8, where $\Gamma_2(q,c)/q^2$ is plotted against the polymer mass concentration c for six scattering angles θ = 10–150°. At smaller θ such as 10° and 30°, the Γ_2/q^2 values are constant for all the c measured.[36] As θ increases, however, the constancy is found to be limited to the smaller c region and the Γ_2/q^2 values begin to decrease with c.[36] The infinite dilution value at finite q, $[\Gamma_2(q,c)/q^2]_{c\to 0}$, was then determined as the average of the constant values in the lower c region. The results are listed in Table II, from which the infinite-dilution Γ_2 value at finite q, $[\Gamma_2(q)]_{c\to 0}$, was estimated. The q dependence of $[\Gamma_2(q)]_{c\to 0}$ is shown in Figure 9 in the form of a Γ_2 vs q plot. The data points seem to tend toward zero as $q \to 0$ and increase rapidly with increasing q. According to the Akcasu theory,[5] the $\Gamma_2(q)$ vs q relation in the small q limit is given for Rouse dynamics by

$$\Gamma_2(q) = G[1 + (1 - Qq^2)^{1/2}] \quad (19a)$$

$$G = \Gamma_2(q=0)/2, \quad Q = 4D_{0,copol}/\Gamma_2(q=0) \quad (19b)$$

which predicts a constant $\Gamma_2(q=0)$ as $q \to 0$, though the

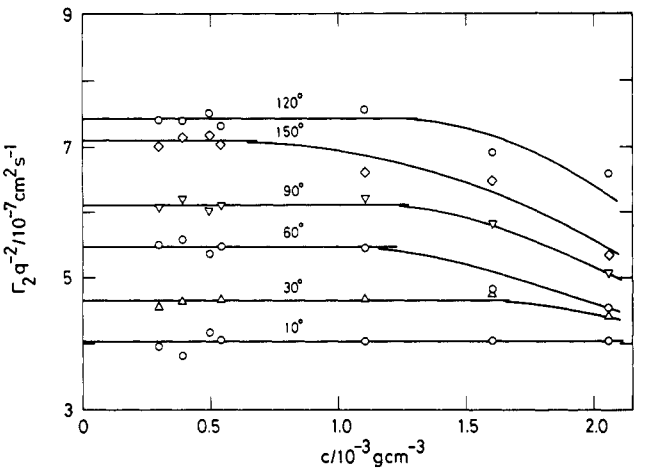

Figure 8. Mean decay rate of the fast mode 2, Γ_2/q^2, plotted against the concentration c for the PS–PMMA diblock copolymer in benzene at 30 °C at six scattering angles ranging from 10° to 150°. The data points at $c = 2.06 \times 10^{-3}$ g cm^{-3}, which will be discussed in part 2 of this series, are shown here to make clear the decreasing tendency of Γ_2/q^2 with increasing c at larger c.

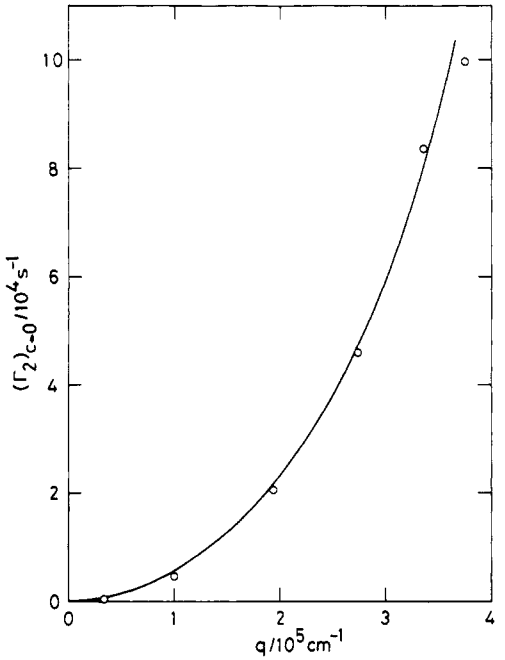

Figure 9. Mean decay rate of the fast mode at infinite dilution, $(\Gamma_2)_{c\to0}$, plotted against q. The fitted solid curve represents an elliptic equation $(\Gamma_2 - G)^2/G^2 + Qq^2 = 1$ with $G = 1.75 \times 10^5$ s^{-1} and $Q = (1/4.0 \times 10^5)^2$ cm^2.

amplitude $a_2(q)$ is expected to vanish as $q \to 0$. Equation 19 represents an upper quarter ($\Gamma_2 \geq G, q \geq 0$) of an elliptic equation, $[\Gamma_2(q) - G]^2/G^2 + Qq^2 = 1$, with its center at $\Gamma_2 = G$, $q = 0$, and with the axial lengths G and $(1/Q)^{1/2}$ for the Γ_2 and q axes, respectively: $\Gamma_2(q)$ is a decreasing function of q^2 near $q \simeq 0$, i.e., $\Gamma_2(q) \simeq \Gamma_2(0) - D_{0,\text{copol}}q^2$. Since the amplitude a_2 is predicted to vanish as $q \to 0$, it may be difficult to detect the constancy of Γ_2 at $q = 0$. However, the prediction of eq 19 differs from the experimental $\Gamma_2(q)$ feature given in Figure 9, where the Γ_2 data increase with q and resemble a lower quarter ($\Gamma_2 \leq G$, $q \geq 0$) of the above-mentioned ellipse in shape, i.e., $\Gamma_2(q) = G[1 - (1 - Qq^2)^{1/2}]$. Actually the $\Gamma_2(q)$ data can be well fitted by an ellipse with $G = 1.75 \times 10^5$ s^{-1} and $Q = (1/4.0 \times 10^5)^2$ cm^2, as is indicated by the solid curve in Figure 9. This leads to the fitting values $[D_{0,\text{copol}}]_{\text{fit}} = 5.5 \times 10^{-7}$ cm^2 s^{-1} and $[\Gamma_2(0)]_{\text{fit}} = 3.5 \times 10^5$ s^{-1}, the former being far from the experimental value $D_{0,\text{block}} = 1.13 \times 10^{-7}$ cm^2 s^{-1}.

It is interesting to point out that, although the experimental $[\Gamma_2(q)]_{c\to0}$ values seem to tend to zero as $q \to 0$

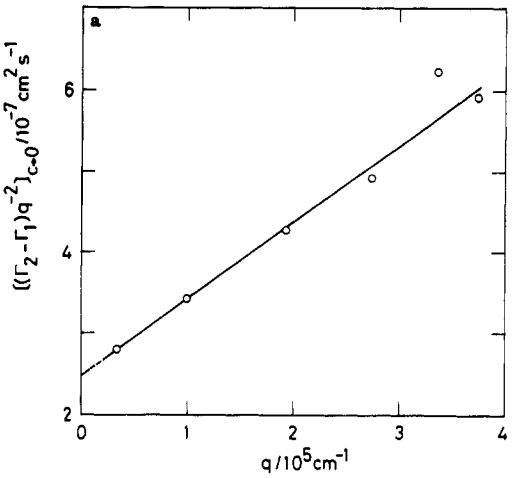

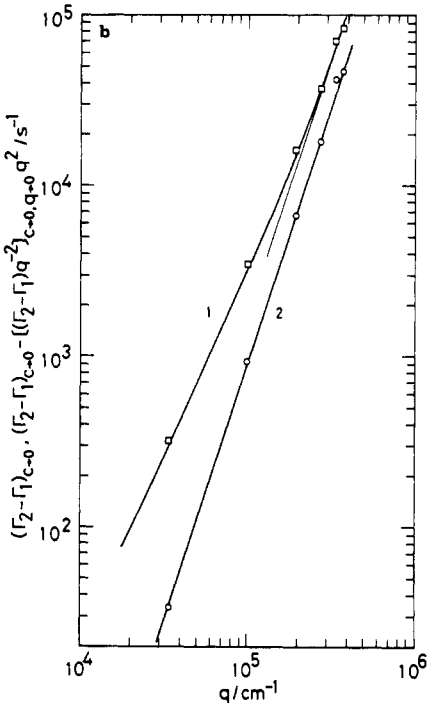

Figure 10. (a) Plots of the modified mean-decay rate $[(\Gamma_2 - \Gamma_1)/q^2]_{c\to0}$ against q for the PS–PMMA diblock copolymer in benzene at 30 °C. (b) Logarithmic plots of the modified mean-decay rate of the fast mode at infinite dilution as a function of q: (□) and curve 1 for $(\Gamma_2-\Gamma_1)_{c\to0}$; (○) and line 2 for $\{(\Gamma_2-\Gamma_1)_{c\to0} - [(\Gamma_2-\Gamma_1)/q^2]_{c\to0,q\to0}q^2\}$. The asymptotic slope of curve 1 at large q is 3; meanwhile line 2 is a straight line with a slope of 3.

(Figure 9), the modified values $[\Gamma_2(q)/q^2]_{c\to0}$ or $\{[\Gamma_2(q) - \Gamma1(q)]/q^2\}_{c\to0}$, which we abbreviate as $\{[\Gamma_{2\text{-}1}(q)]/q^2\}_{c\to0}$, give a nonzero value when they are plotted against q and are extrapolated linearly to $q \to 0$. Figure 10a shows this situation, where $\{[\Gamma_{2\text{-}1}(q)]/q^2\}_{c\to0}$ is plotted as a function of q. The plot gives the intercept $(\Gamma_{2\text{-}1}/q^2)_{c\to0,q\to0} = 2.50 \times 10^{-7}$ cm^2 s^{-1} at $q = 0$ and indicates q^3 dependence. Then, as shown by solid line 2 in Figure 10b, the modified values $\{[(\Gamma_{2\text{-}1}(q)]_{c\to0} - [(\Gamma_{2\text{-}1})/q^2]_{c\to0,q\to0}q^2\}$ are well expressed by a straight line of slope 3 over the whole q range measured and are represented by a relation

$$(\Gamma_{2\text{-}1})_{c\to0} = [(\Gamma_{2\text{-}1})/q^2]_{c\to0,q\to0}q^2 + 9.03 \times 10^{-13}q^3 \text{ (s}^{-1}\text{)} \quad (20a)$$

$$[(\Gamma_{2\text{-}1})/q^2]_{c\to0,q\to0} = 2.50 \times 10^{-7} \text{ (cm}^2\text{ s}^{-1}\text{)} \quad (20b)$$

In contrast, the values $[\Gamma_{2\text{-}1}(q)]_{c\to0}$, shown in Figure 10b, tend toward a limiting line of slope 3 only at large q as demonstrated by solid line 1. Benmouna et al.[20] have predicted with the random-phase approximation or the

mean-field approximation that mode 2 is a relaxation mode characteristic of block copolymer chains (which was called a copolymer mode) and that its decay rate $[\Gamma_2(q)]_{c\to 0}$ becomes constant at small q, while it gives the familiar q^4 Rouse behavior in the intermediate-q region if the Gaussian chain nature without hydrodynamic interactions (free-draining, FD) is assumed for both block subchains: 50/50 diblock copolymers, for example, give

$$(\Gamma_2)_{c\to 0} = 3D_{0,\text{homo-A}}/R_G^2 \quad (qR_G \ll 1, \text{FD}) \tag{21a}$$

$$= (1/12)(k_BT/\zeta a^2)(qa)^4 \quad (qR_G \gg 1, \text{FD}) \tag{21b}$$

with ζ and a the friction constant and the statistical unit length, respectively, of the monomers of the two subchains, both subchains having the same radius of gyration $R_G/2^{1/2}$ and the same number of monomers. Following the procedures of Benmouna et al., we predict for the 50/50 Gaussian diblock chain with nondraining hydrodynamic interactions (ND) that[21]

$$(\Gamma_2)_{c\to 0} = 0.459k_BT/\eta_s R_G^3 \quad (qR_G \ll 1, \text{ND}) \tag{22a}$$

$$= 0.0549q^3/k_BT\eta_s \quad (qR_G \gg 1, \text{ND}) \tag{22b}$$

The q^3 dependence of the experimental $[\Gamma_2(q)]_{c\to 0}$ and $[\Gamma_{2\text{-}1}(q)]_{c\to 0}$ values agrees with the ND behavior of eq 22. This means that the internal motions of the diblock chain suffer strong hydrodynamic interactions. The diffusion-like term $[(\Gamma_{2\text{-}1})/q^2]_{c\to 0,q\to 0}q^2$ obtained experimentally, on the other hand, disagrees with the prediction of a q-independent term in eqs 21, 22, or 15 at $q \to 0$.

The diffusion-coefficient-like value, $[(\Gamma_{2\text{-}1})/q^2]_{c\to 0,q\to 0} = 2.50 \times 10^{-7}$ cm^2 s^{-1} (eq 20), is more than twice as large as D_0 of mode 1 (Table III); the Γ_2 motion is about twice as fast as the entire diblock-chain diffusion. Benmouna et al.[20] first suggested that Γ_2 can be identified with interdiffusion. Recently, however, this suggestion has been recognized not to be true in general;[4,5] the Γ_2 is a complex function including both interdiffusion and cooperative diffusion coefficients. Thus the above-mentioned constant term, $[\Gamma_{2\text{-}1}/q^2]_{c\to 0,q\to 0}$, may not be attributed simply to the relative motion of the collective PS subchain with respect to the collective PMMA subchain in a single block. However, the experimental Γ_2 behavior confirms clearly that active thermal fluctuations in the concentrations of the PS and PMMA subchains play an important role in the dynamics of diblock copolymers in solution, a role which is conspicuous when compared with that of homopolymers. The distance fluctuation between the PS elements which originally happens in the inside of the homo-PS chain is amplified and/or modulated by the dynamical heterocontact effect between the PS–PMMA subchain monomers in the diblock copolymer. This effect, especially in dilute solution, makes the fluctuation in the PS monomer density very large. Such fluctuations help to produce the q^3 dependence in $[\Gamma_{2\text{-}1}(q)]_{c\to 0}$ at large qR_G.

First Cumulant. Figure 11 shows the concentration dependence of the first cumulant Γ_e at given q in the form of Γ_e/q^2. For each q, the Γ_e/q^2 values are expressed well by the linear relation

$$\Gamma_e(q,c)/q^2 = [\Gamma_e(q,c)/q^2]_{c\to 0}[1 + k_\Gamma(q)c] \tag{23}$$

The linear extrapolation of Γ_e/q^2 to zero concentration allows us to estimate both $[\Gamma_e(q,c)]/q^2]_{c\to 0}$ and the slope $k_\Gamma(q)$ at constant q; the slope changes sign drastically from positive to negative with increasing q. These results are listed in Table II, where the small-q limit value $[\Gamma_e(q,c)/q^2]_{c\to 0,q\to 0} = 1.13 \times 10^{-7}$ cm^2 s^{-1} is also given. The first cumulant Γ_e of the scattering function for the visible PS subchain represents the short-time behavior of the chain and can be expressed by both the mobility and the static structure factor of the PS part. The small-q limit of $\Gamma_e(q)/q^2$ defines the short-time diffusion coefficient. $[\Gamma_e(q,c)/q^2]_{c\to 0,q\to 0}$ is then expected theoretically to approach the translational diffusion coefficient of the PS subchain, $D_{0,\text{homo-PS}}$,[4,5,7] not the long-time one representing the motion of the entire copolymer molecule, $D_{0,\text{copol}}$, with $D_{0,\text{homo-PS}} > D_{0,\text{copol}}$.[3,4] Experimentally $D_{0,\text{copol}}$ is considered to be $D_{0,\text{block}} = [\Gamma_1/q^2]_{c\to 0,q\to 0}$. The results in Table II show that the inequality relation $\Gamma_e/q^2 > \Gamma_1/q^2$ is realized at small q at every concentration c measured and that it reaches the equality $(\Gamma_e/q^2)_{c\to 0,q\to 0} = (\Gamma_1/q^2)_{c\to 0,q\to 0} = 1.13 \times 10^{-7}$ cm^2 s^{-1} at $c \to 0$ and $q \to 0$. The last value obtained is just $D_{0,\text{block}}$, and not equal to $D_{0,\text{homo}} = 1.59 \times 10^{-7}$ cm^2 s^{-1} (Table III). The difference between the two D_0 values is due mainly to the vast deformation of the copolymer chain during diffusion and gives us information on the peculiar internal copolymer motions in solution.

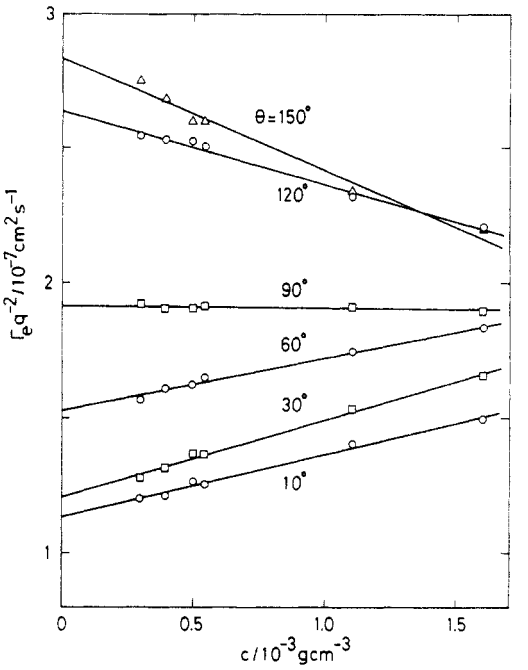

Figure 11. Concentration dependence of the first cumulant Γ_e/q^2 for the PS–PMMA diblock copolymer in benzene at 30 °C at six scattering angles of 10–150°.

In Figure 12 the $(\Gamma_e)_{c\to 0}/D_0q^2$ values at finite q are plotted logarithmically versus qR_G with $D_0 = D_{0,\text{block}}$ and $R_G = R_{G,\text{block}}$. The data points (unfilled circles) are constant (unity) at small qR_G and approach a limiting line of slope 1, i.e., the nondraining q^3 dependency, with increasing qR_G. It is very impressive that the limiting behavior is found to appear at a fairly early stage of the intermediate qR_G region. According to a very recent renormalization-group treatment by Shiwa[22] of flexible linear chain dynamics in solution, $(\Gamma_e)_{c\to 0}/D_0q^2$ is a true universal function depending only on qR_G. Curve S in the figure represents the theoretical behavior for a swollen chain in the good solvent limit, i.e., for a self-avoiding walk with a nonpreaveraged Oseen tensor.[22,23] Very quick approach of the present $(\Gamma_e)_{c\to 0}/D_0q^2$ data to the q^3 region is made clear. This feature can also be confirmed by comparing the present data with the previous one obtained by us for homopolymer chains in good solvents.[15,18] Figure 13 visualizes the circumstances; in the case of the present PS–PMMA diblock chain (unfilled triangles), the rise of $(\Gamma_e)_{c\to 0}/D_0q^2$ starts at much smaller qR_G than for polyisoprene (PIP, unfilled circles)[18] and for PS (filled circles).[15] Thus, the fluctuation of the PS-subchain motions, which is activated by the PS–PMMA heterocontacts, causes the

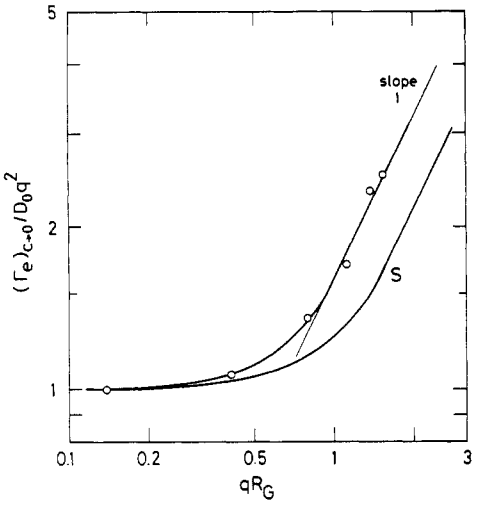

Figure 12. First cumulant at infinite dilution $(\Gamma_e)_{c\to0}/D_0q^2$ plotted against qR_G in the logarithmic scales: (○) the present data for the PS–PMMA diblock copolymer in benzene at 30 °C, approaching the asymptotic slope 1 at larger qR_G. Here D_0 and R_G denote $D_{0,block}$ and $R_{G,block}$, respectively. Curve S represents the theoretical prediction made for the homopolymer chain of the self-avoiding walk with a nonpreaveraged Oseen tensor.[22,23]

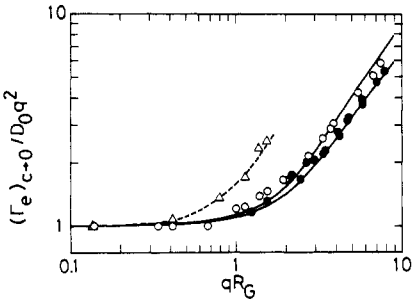

Figure 13. Comparison of the first cumulant $(\Gamma_e)_{c\to0}/D_0q^2$ versus qR_G relations between the present PS–PMMA diblock copolymer and the homopolymers in good solvents: (△) the present data; (○) polyisoprene (PIP) data in cyclohexane at 25 °C;[18] (●) PS data in benzene at 30 °C.[15]

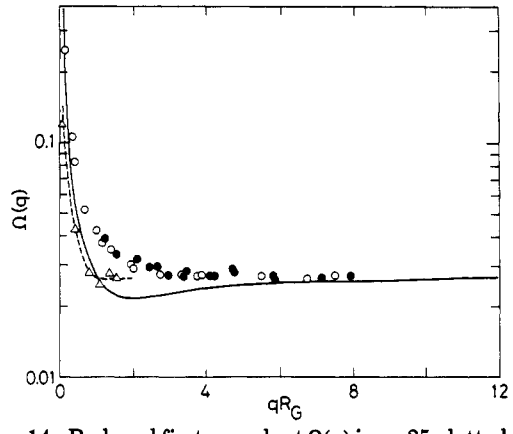

Figure 14. Reduced first cumulant Ω(q) in eq 25 plotted against qR_G in the logarithmic scales: (△) the present PS–PMMA diblock copolymer data in benzene at 30 °C; (○) PIP data in cyclohexane at 25 °C;[18] (●) PS data in benzene at 30 °C.[15] The solid curve is the theoretical line calculated for the nondraining homopolymer chain with a nonpreaveraged Oseen tensor.[22]

$(\Gamma_e)_{c\to0}/D_0q^2$ values to rise even at $qR_G \simeq 0.4$ and to reach the asymptotic q^3 behavior near $qR_G \simeq 1$. The asymptotic coefficient at $qR_G \gg 1$, i.e., the value C in the relation $[\Gamma_e(q=\infty)]_{c\to0}/D_0q^2 = CqR_G$, is 1.63, which is much larger than the theoretical one, 1.283, given by Shiwa and Tsunashima.[2,23]

Figure 14 shows the qR_G dependence of the reduced first cumulant Ω(q) (see eq 25). Here the unfilled triangles are the data on the present PS–PMMA diblock copolymer, and unfilled and filled circles are our previous data on homopolymer–good solvent systems, PIP in cyclohexane[18] and PS in benzene,[15] respectively. According to the theoretical analysis of Shiwa,[22] the usual reduced first cumulant $\Gamma^*(q)$

$$\Gamma^*(q) \equiv \eta_s[\Gamma_e(q,c)]_{c\to0}/k_BTq^3 \tag{24}$$

is discarded here because of its lack of universality, and a revised one Ω(q) is adopted instead;

$$\Omega(q) \equiv \eta_e[\Gamma_e(q,c)]_{c\to0}/k_BTq^3, \quad \Omega(q=\infty) = 0.02669 \tag{25}$$

$$\Gamma^*(q) = \lambda_0^2\Omega(q), \quad \lambda_0^2 \equiv \eta_s/\eta_e \tag{26}$$

Here Ω becomes a universal function of qR_G only after taking into account the local solvent viscosity in the neighborhood of a polymer chain, η_e. The parameter λ_0 represents the difference between η_e and the bulk solvent viscosity η_s and is a measure of the strength of dynamical polymer–solvent coupling. The solid curve in Figure 14 represents the theoretical Ω versus qR_G relation. For the present data on the PS–PMMA diblock copolymer, we estimated λ_0 to be 1.95,[24] which is very close to the previous λ_0 values on PIP and PS in Θ solvents.[2] With this λ_0 value, the present Ω(q) values are found to decrease rapidly with increasing qR_G and then reach an asymptotic constant, 0.02669 (eq 25), in the surprisingly small qR_G region, as is shown by a broken curve in Figure 14. The constancy of Ω(q) confirms the nondraining nature of the present diblock chain, but its trend to the constant value is very drastic when compared with flexible linear chains. For linear chains, their data can also be represented well by a master curve irrespective of the polymer species, as is predicted theoretically[22] and is shown in the figure, but the trend to the constant limit is slow. The first cumulant, by definition in eq 6, contains all the dynamical fluctuation motions in the chain. The sharp decrease in Ω shown by the broken line might indicate that the block copolymer may retain many internal modes of motion that are not relaxed in the small-t limit.

Concentration Dependence of $D(c)$ and $\Gamma_e(q,c)$. In the previous sections, we discussed active intramolecular motions in the block chain. We will refer in this section to the intermolecular interactions in terms of the concentration dependence of D and Γ_e. The concentration coefficient of the diffusion coefficient of the present diblock molecule, i.e., k_D in eq 12, was obtained to be $k_D = 113$ cm^3 g^{-1}, as already described. k_D is a quantity which is influenced by the interchain thermodynamic (the excluded-volume effect) and hydrodynamic interactions. It is thus useful to discuss k_D with the hydrodynamic-based volume-fraction coefficient k_D^V;[5,6,25,26]

$$k_D^V \equiv k_D/(N_AV_H/M) \tag{27}$$

where V_H is the equivalent hydrodynamic volume of the chain defined by $V_H \equiv (4\pi/3)R_H^3$. In Figure 15, the present data point is shown by an unfilled triangle as the function of the dimensionless parameter $\bar{X}$, together with our previous data on homopolymers, PIP (unfilled circles) and PS (filled circles) in good solvents.[18] The data at Θ temperature[27,28] are also shown at $\bar{X} = 0$. Here $\bar{X}$ represents the strength of the thermodynamic and hydrodynamic interactions and is expressed by the ratio of the equivalent thermodynamic radius $\bar{S}$, which is defined through the second virial coefficient A_2 as $\bar{S} \equiv [A^2/(16\pi N_A/3M^2)]^{1/3}$, to the hydrodynamic radius R_H;

$$\bar{X} \equiv \bar{S}/R_H \tag{28}$$

It is found from the figure that the present data point is

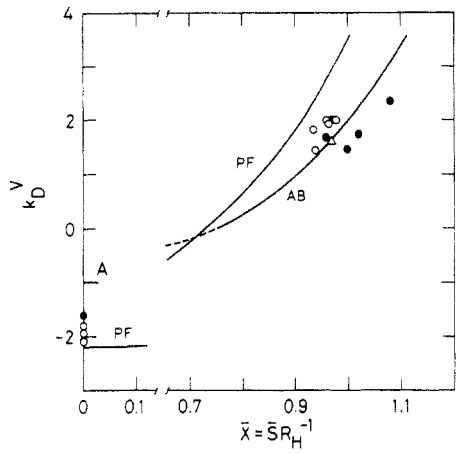

Figure 15. Concentration coefficient of the diffusion coefficient expressed in the volume-fraction frame, k_D^V in eq 27, plotted against the dimensionless size parameter $\bar{X}$ (in eq 28): (Δ) the present PS–PMMA diblock copolymer data in benzene at 30 °C; (○) PIP data in cyclohexane at 25 °C[17] and in 1,4-dioxane at 34.7 °C (θ temperature; i.e., $\bar{X} = 0$);[28] (●) PS data in benzene at 30 °C[17] and in *trans*-decalin at 20.4 °C (θ temperature).[27] The solid curves are the theoretical ones: AB curve in good solvents by Akcasu and Benmouna;[25] A curve in θ solvents by Akcasu et al.;[6] PF curve by Pyun and Fixman.[29]

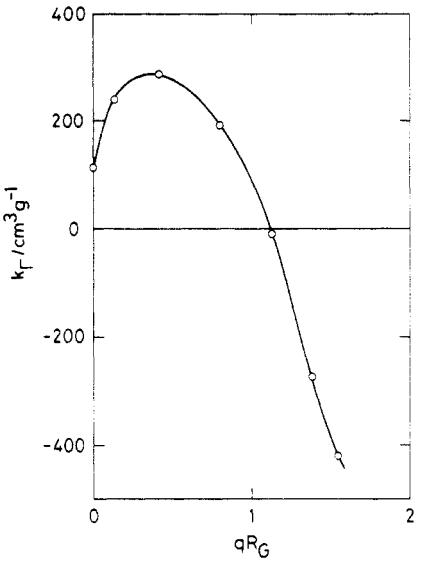

Figure 16. Concentration coefficient of the first cumulant, k_Γ, plotted against qR_G for the PS–PMMA diblock copolymer in benzene at 30 °C.

located well on the theoretical line AB, which was first obtained by Akcasu and Benmouna[25] for homopolymers and then improved by Akcasu et al.[6] for the visible components in multicomponent polymer solutions;

$$k_D^V = 8\bar{X}^3 - 6\bar{Y}^2 = \bar{X}^2(8\bar{X} - 6)$$

(AB, good solvent limit[25]) (29a)

$$= -6\bar{Y}^2 \simeq -1$$

(A, θ solvent limit[6]) (29b)

where $\bar{Y}$ is related to the first moment of the pair distribution function of a pair of visible subchains, whereas $\bar{X}$ involves the second moment. In the good solvent limit, $\bar{Y} \simeq \bar{X}$ with use of a hard-sphere model for the pair distribution function[6] and leads to the AB formula in eq 29a. The expression $k_D \simeq -1$ at the θ point comes from Monte Carlo numerical calculations of $\bar{Y}$.[6] On the other hand, the line PF in Figure 15 represents the Pyun–Fixman equation[29]

$$k_D^V = 8\bar{X}^3 - 7.16 + K \quad \text{(PF)} \qquad (30)$$

where the quantity K becomes zero in the good solvent limit. The present k_D, which was observed for the visible PS subchains, thus agrees completely with the behavior of homopolymer chains in good solvents.[30-32] The PF theory explains well the data in θ solvents.[27,28]

The concentration coefficient of the first cumulant, $k_\Gamma(q)$ in eq 23, at given q for the present PS–PMMA block chain was estimated from the data shown in Figure 11 and is plotted against qR_G in Figure 16. The k_Γ values are positive at $qR_G < 1$ but take a maximum around $qR_G \simeq {}^1/_2$ and then decrease sharply with increasing qR_G, going down to negative values at $qR_G > 1$. Positive k_Γ and its decrease with increasing qR_G was predicted theoretically for flexible linear chains by Hammouda and Akcasu[33] but a negative k_Γ was not. Negative k_Γ has first been observed for a block copolymer, polystyrene–polybutadiene diblock copolymer, in a selective solvent[34] where micellar formation occurs. The positive k_Γ in the present study is attributed to the positive k_D ($=k_\Gamma(q=0)$ = 113 cm^3 g^{-1}) of the translational diffusion motion of the block chain (mode 1). The negative k_Γ is, on the other hand, due to the concentration fluctuation of the PS and PMMA elements in the block chain, i.e., the copolymer mode, which induces the active internal modes of motion. This mode might produce net attractive (negative) interactions between the PS parts of different chains. These two effects will thus concur to produce a maximum on the curve of the k_Γ versus qR_G plot.

Thermodynamic intermolecular interactions between the block chains also affect k_D and k_Γ behavior; e.g., the thermodynamic relation, $k_D + k_s = 2A_2M$, holds well, where k_s is the coefficient of the concentration dependence of the sedimentation coefficient. Table I shows that the present diblock chain has positive A_2 and negative A_3. This result will give us some suggestions not only on the PS–PS and PMMA–PMMA subchain interactions but also on the PS–PMMA heterosubchain interactions. Kimura and Kurata have discussed just A_2 of block chains in the presence of the heterosubchain interactions.[35] However, there was no prediction on A_3. More theoretical and experimental works will be needed on thermodynamic and hydrodynamic interactions in diblock copolymer chains.

References and Notes

(1) For example: (a) Akcasu, A. Z.; Benmouna, M.; Han, C. C. *Polymer* **1980**, *21*, 866. (b) Schaefer, D. W.; Han, C. C. *Dynamic Light Scattering*; Pecora, R., Ed.; Plenum: New York, 1985; Chapter 5.
(2) Tsunashima, Y. *Polym. J.* **1992**, *24*, 433.
(3) Akcasu, A. Z. *Macromolecules* **1982**, *15*, 1321.
(4) Akcasu, A. Z.; Nägele, G.; Klein, R. *Macromolecules* **1991**, *24*, 4408.
(5) Akcasu, A. Z. *Dynamic Light Scattering. The Method and Some Applications*; Brown, W., Ed.; Clarendon: Oxford, U. K., 1993; Chapter 1.
(6) Akcasu, A. Z.; Hammouda, B.; Lodge, T. P.; Han, C. C. *Macromolecules* **1984**, *17*, 759.
(7) Burchard, W.; Kajiwara, K.; Nerger, D.; Stockmayer, W. H. *Macromolecules* **1984**, *17*, 222.
(8) Tsunashima, Y.; Hirata, M.; Kawamata, Y. *Macromolecules* **1990**, *23*, 1089.
(9) Utiyama, H.; Takenaka, K.; Mizumori, M.; Fukuda, M.; Tsunashima, Y.; Kurata, M. *Macromolecules* **1974**, *7*, 515.
(10) Tsunashima, Y. Proceedings of the 27th Europhysics Conference on Macromolecular Physics, 1991. The molecular weights in ref 9 were checked again, and all the data were then reanalyzed.
(11) Utiyama, H.; Takenaka, K.; Mizumori, M.; Fukuda, M. *Macromolecules* **1974**, *7*, 28.
(12) Nemoto, N.; Tsunashima, Y.; Kurata, M. *Polym. J.* **1981**, *13*, 827.
(13) Tsunashima, Y.; Nemoto, N.; Kurata, M. *Macromolecules* **1983**, *16*, 584.

(14) Kurata–Kimura theory (*J. Polym. Sci., Polym. Phys. Ed.* **1979**, *17*, 2133) had discussed the chain conformation of AB diblock copolymers in a dilute solution in terms of the thermodynamic interactions between the block subchains. It predicted that, in good solvents for both A and B subchains, the AB diblock chains expand much more than the homopolymer chains do if the repulsive intrasegmental interactions work between not only A–A and B–B but also A–B and if the former is much stronger than the latter.
(15) Nemoto, N.; Tsunashima, Y.; Kurata, M. *Macromolecules* **1984**, *17*, 425.
(16) Fukuda, M.; Fukutomi, M.; Kato, Y.; Hashimoto, T. *J. Polym. Sci., Polym. Phys. Ed.* **1974**, *12*, 871.
(17) Tsunashima, Y.; Nemoto, N. *Macromolecules* **1984**, *17*, 2931.
(18) Tsunashima, Y.; Hirata, M.; Nemoto, N.; Kurata, *M. Macromolecules* **1987**, *20*, 1992.
(19) (a) Utiyama, H.; Tsunashima, Y.; Kurata, M. *J. Chem. Phys.* **1971**, *55*, 3133. (b) Tsunashima, Y.; Kurata, M. *J. Chem. Phys.* **1986**, *84*, 6432.
(20) Benmouna, M.; Benoit, H.; Borsali, R.; Duval, M. *Macromolecules* **1987**, *20*, 2620.
(21) Tsunashima, Y. Unpublished calculations.
(22) Shiwa, Y. *J. Phys. A: Math. Gen.* **1991**, *24*, L579.
(23) Shiwa, Y.; Tsunashima, Y. *Physica A*, in press.
(24) The λ_0 value was obtained from eq 26 by adjusting the experimental asymptotic value, $\Gamma^*(q=\infty) = 0.1017$, to the theoretical one $\Omega(q=\infty) = 0.02669$.
(25) Akcasu, A. Z.; Benmouna, M. *Macromolecules* **1978**, *11*, 1193.
(26) Akcasu, A. Z. *Polymer* **1981**, *22*, 1169.
(27) Tsunashima, Y.; Nemoto, N. *Macromolecules* **1983**, *16*, 1941.
(28) Tsunashima, Y.; Hirata, M.; Nemoto, N.; Kajiwara, K.; Kurata, M. *Macromolecules* **1987**, *20*, 2862.
(29) Pyun, C. W.; Fixman, M. *J. Chem. Phys.* **1964**, *41*, 937.
(30) Han, C. C.; Akcasu, A. Z. *Polymer* **1981**, *22*, 1165.
(31) van der Berg, H.; Jamieson, A. M. *J. Polym. Sci., Polym. Chem. Ed.* **1983**, *21*, 2311.
(32) Huber, K.; Burchard, W.; Akcasu, A. Z. *Macromolecules* **1985**, *18*, 2743.
(33) Hammouda, B.; Akcasu, A. Z. *Macromolecules* **1983**, *16*, 1852.
(34) Tsunashima, Y. *Macromolecules* **1990**, *23*, 2963.
(35) Kimura, T.; Kurata, M. *Macromolecules* **1981**, *14*, 1104.
(36) In order to clarify the decrease in the values with increasing c, data points at $c = 2.06 \times 10^{-3}$ g cm^{-3} are also shown in the same figure.